Harmonically confined Tonks-Girardeau gas: A simulation study based on Nelson's stochastic mechanics

W. Paul*
Institute of Physics, Martin-Luther-University, 06099 Halle, Germany
(Received 16 May 2012; published 6 July 2012)

We present a simulation study of the properties of the Tonks-Girardeau gas, a system of N hard-core bosons confined in a one-dimensional harmonic trap. For this system the ground-state wave function is exactly known based on a Bose-Fermi mapping theorem. We employ Nelsons' interpretation of quantum mechanics in which this N-body wave function gives rise to a set of stochastic differential equations for the positions of the N particles, which can be simulated by standard methods. In particular, real space densities and momentum distributions can simply be determined by time averages along particle trajectories. Employing this approach we are able to significantly extend the range of particle numbers N treated numerically compared to earlier approaches, while reproducing all exactly known results for this model. We also show that for the bosons in a harmonic trap, contrary to what has been assumed so far, the momentum distribution reflects the system size scaling of the occupation numbers of the natural orbitals; that is, it can be used to decide on the presence of a Bose-Einstein condensate.

DOI: 10.1103/PhysRevA.86.013607 PACS number(s): 67.85.Bc, 03.65.Ta, 02.50.Ey

I. INTRODUCTION

Ultracold quantum gases have received much attention in the last fifteen years [1] because they allowed, on the one hand, for the realization of Bose-Einstein condensates (see, e.g., Refs. [2–5]) and, on the other hand, for the creation of strongly correlated quantum fluids [6–8]. While the first class of system can be well described within quasiparticle concepts [5] and on the basis of a mean-field type approach [9], the latter is characterized by strong correlation effects [1,10]. Theoretically, [11–14], strongly correlated one-dimensional bosonic gases have been discussed long before they could be realized experimentally [6–8].

Besides providing model systems for condensed matter physics [1] the quantum mechanical correlation effects present in these systems provide testing grounds to advance our understanding of quantum systems and our abilities to treat them theoretically and numerically. The one-dimensional Tonks-Girardeau gas [11] is of particular interest because it is amenable to an exact solution for the N-particle ground-state wave function (see the presentation in the next section). However, many relevant properties of this strongly correlated bosonic system are only obtainable by sophisticated numerical analysis based on that known solution [15–17].

A numerical approach which in principle provides a complete microscopic picture of such quantum systems is based on Nelson's stochastic mechanic approach to nonrelativistic quantum mechanics [18,19]. While this approach has been used to study fundamental quantum phenomena such as, for example, the double-slit experiment [20] or tunneling processes [21], it has not been tried yet for the Tonks-Girardeau gas. Nelson derived the Schrödinger equation starting by analyzing the kinematic properties of conservative diffusion processes. He showed that to each solution of the Schrödinger equation corresponds a stochastic differential equation for the quantum particles described by such a wave function, similar to the correspondence between a solution to the Hamilton-Jacobi equation and Newton's equation in classical mechanics. This approach therefore offers a possibility to realize an ensemble of paths for the quantum system under study and to determine quantum mechanical observables from the properties of this ensemble of paths.

In the next section we will provide some theoretical background on the Tonks-Girardeau gas as well as on Nelson's stochastic mechanics approach to quantum mechanics. In Sec. III we will then discuss our results for the properties of the Tonks-Girardeau gas confined in a harmonic external potential, while Sec. IV provides some conclusion and outlook. An appendix finally provides some details about the numerical simulations.

II. THEORY AND SIMULATION APPROACH

We consider a one-dimensional system of N hard bosons with diameter a in a harmonic trapping potential. The Hamiltonian thus reads

$$\tilde{H} = \sum_{i=1}^{N} \left(-\frac{\hbar^2}{2m} \frac{\partial^2}{\partial \tilde{x}_i^2} + \frac{1}{2} m\omega^2 \tilde{x}_i^2 \right). \tag{1}$$

The hard-core interaction between the bosons is most conveniently treated as a constraint on the wave function

$$\tilde{\psi} = 0 \text{ if } |\tilde{x}_i - \tilde{x}_j| < a, \quad 1 \leqslant i \leqslant j \leqslant N. \tag{2}$$

We will discuss this model in scaled variables $x_i = \tilde{x}_i/\sqrt{\hbar/m\omega}$ and $H = H/(\hbar\omega)$.

$$H = \sum_{i=1}^{N} \left(-\frac{1}{2} \frac{\partial^2}{\partial {x_i}^2} + \frac{1}{2} {x_i}^2 \right) \tag{3}$$

and $\psi(x_1, \ldots, x_N) = \tilde{\psi}(\tilde{x}_1, \ldots, \tilde{x}_N)$. Evoking the Fermi-Bose mapping theorem [11] the N-boson ground state is given through the ground state of a fictitious spinless N-fermion system with the same Hamiltonian and constraint as

$$\psi_B(x_1, \ldots, x_N) = |\psi_F(x_1, \ldots, x_N)|. \tag{4}$$

*Wolfgang.Paul@Physik.Uni-Halle.De

When one considers dilute systems, one can perform the limit $a \to 0$. In the spinless fermionic system the constraint $\psi(x_1,\ldots,x_i,\ldots,x_j,\ldots,x_N) = 0$ if $x_i = x_j$ for arbitrary $1 \leqslant i \leqslant j \leqslant N$ is automatically fulfilled, so the problem reduces to the determination of the ground-state wave function of N noninteracting, spinless fermions. The solution is, of course, given by a Slater determinant of the single-particle eigenfunctions of the harmonic oscillator. Girardeau *et al.* [22] have shown that this solution can be expressed as

$$\psi_B(x_1,\ldots,x_N) = C_N \prod_{i=1}^{N} e^{-\frac{x_i^2}{2}} \prod_{1\leqslant j\leqslant k\leqslant N} |x_k - x_j|. \quad (5)$$

The normalization constant is given by

$$C_N = 2^{N(N-1)/4}\left[N!\prod_{n=0}^{N-1} n!\sqrt{\pi}\right]^{-1/2}. \quad (6)$$

The ground-state density for this highly correlated bosonic system can thus be given exactly based on the mapping to to the spinless fermions. The N bosons occupy the N lowest single-particle eigenstates of the harmonic oscillator, $\phi_n(x)$; that is, we have

$$\begin{aligned}\rho_1(x) &= N\int |\psi_B(x,x_2,\ldots,x_N)|^2 dx_2\cdots dx_N \\ &= \sum_{n=0}^{N-1}|\phi_n(x)|^2 = \frac{1}{\sqrt{\pi}}\sum_{n=0}^{N-1}\frac{1}{2^n n!}H_n^2(x)e^{-x^2}, \end{aligned} \quad (7)$$

where $H_n(x)$ is the nth order Hermite polynomial [22,23]. This function shows pronounced deviations from a mean-field description based on the Gross-Pitaevskii equation [23,24], underlining the strong correlation effects in this one-dimensional boson system. Its overall shape, however, can still be captured in a Thomas-Fermi type mean-field theory [23] and the deviations from it can also be obtained [25,26]. More interesting as far as correlation effects are concerned is the reduced single-particle density matrix

$$\begin{aligned}\rho_1(x,x') = N\int dx_2\cdots dx_N \psi_B(x,x_2,\ldots,x_N) \\ \times \psi_B(x',x_2,\ldots,x_N). \end{aligned} \quad (8)$$

For a nontrivial number N of trapped bosons, this function is only numerically accessible. Its eigenfunctions and eigenvalues define the natural orbitals (effective single-particle states) and their occupation numbers; we will discuss that in more detail in the results section. The single-particle density matrix also is related to the momentum distribution of the bosons by

$$n(k) = \frac{1}{2\pi}\int_{-\infty}^{\infty} dx \int_{-\infty}^{\infty} dx' \rho_1(x,x') e^{-ik(x-x')}. \quad (9)$$

It has been shown by Olshanii and Dunjko [27] and Moreno [28] that, independent of the trapping potential, this distribution function asymptotically behaves as $n(k) \simeq k^{-4}$ for $k \to \infty$. For $N = 2$ the prefactor for this law is known [29]. For general N this prefactor, as well as the complete function $n(k)$, has to be determined numerically. As this involves the numerical evaluation of high-dimensional integrals, this was mostly done for $N \leqslant 10$ [30,31]; however, in Ref. [15] a Monte Carlo integration method based on the Gaussian unitary ensemble was used to calculate the momentum distribution up to $N = 160$.

In the following we will address the numerical evaluation of the properties of this harmonically trapped boson system employing the tools offered by Nelson's stochastic mechanics approach to quantum mechanics [18,19]. In this approach, a given solution $\psi(y,\tilde{t}) = \exp[R(y,\tilde{t}) + \frac{i}{\hbar}S(y,\tilde{t})]$ of the Schrödinger equation corresponds to a set of possible paths $y(\tilde{t})$ obeying the following stochastic differential equation:

$$dy(\tilde{t}) = \frac{\hbar}{m}\left(\frac{d}{dy}R(y,\tilde{t}) + \frac{1}{\hbar}\frac{d}{dy}S(y,\tilde{t})\right)d\tilde{t} + \sqrt{\frac{\hbar}{m}}dW(\tilde{t}), \quad (10)$$

with the Gaussian Wiener process $dW(\tilde{t})$ with first two moments

$$\langle dW(\tilde{t})\rangle = 0 \quad \text{and} \quad \langle dW(\tilde{t})dW(\tilde{t}')\rangle = \delta(\tilde{t}-\tilde{t}') = d\tilde{t}. \quad (11)$$

This stochastic differential equation describes a conservative (in the mean) diffusion process with sample paths distributed around the classical trajectory given by

$$dy_{cl}(\tilde{t}) = \frac{1}{m}\frac{d}{dy}S(y,\tilde{t})d\tilde{t} = v_{cl}d\tilde{t}. \quad (12)$$

For our system we obtain from Eq. (5):

$$S(x_1,\ldots,x_N) = 0, \quad (13)$$

$$R(x_1,\ldots,x_N) = \ln(C_N) - \sum_{i=1}^{N}\frac{x_i^2}{2} + \sum_{1\leqslant j\leqslant k\leqslant N}\ln|x_k - x_j|. \quad (14)$$

The quantity

$$u_i(x_1,\ldots,x_N) = \frac{d}{dx_i}R(x_1,\ldots,x_N) \quad (15)$$

is the so-called osmotic velocity [18] of particle i, $mu_i(x_1,\ldots,x_N)$ is the random variable which is the stochastic mechanic equivalent of the quantum mechanical momentum of particle i.

For our system, the resulting stochastic differential equations generating the paths of the hard bosons read in normalized coordinates, introducing also a scaled time variable $t = \omega\tilde{t}$,

$$dx_i(t) = \left[-x_i + \sum_{j=1,j\neq i}^{N}\frac{\mathrm{sgn}(x_j - x_i)}{|x_j - x_i|}\right]dt + dW_i(t). \quad (16)$$

The numerical approach to integrate this equation will be discussed in the appendix. In the next section we present our results.

III. RESULTS

We want to stress at the outset of this section that all results shown in the following have been obtained by treating the system of N hard-core bosons described by the equation of motion (16) as a classical N-particle system for which, for example, a real-space density and momentum distribution can be obtained by time averaging over instantaneous positions and momenta.

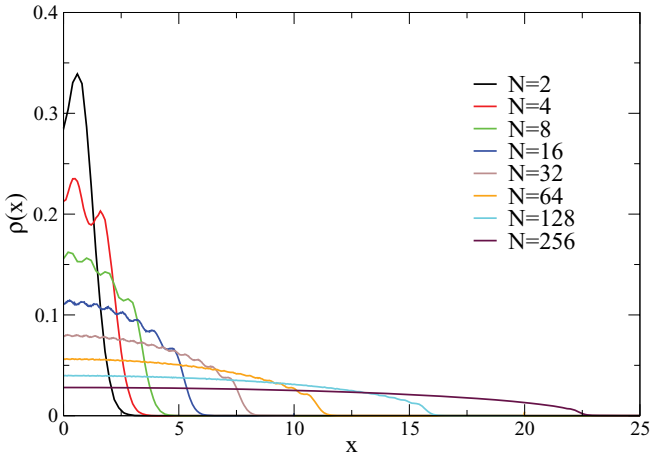

FIG. 1. (Color online) Probability to find a particle at position x for different numbers of bosons indicated in the legend. Only the positive half of the function which is symmetric around $x = 0$ is shown. The extent of the distribution increases monotonically with growing N while its amplitude decreases.

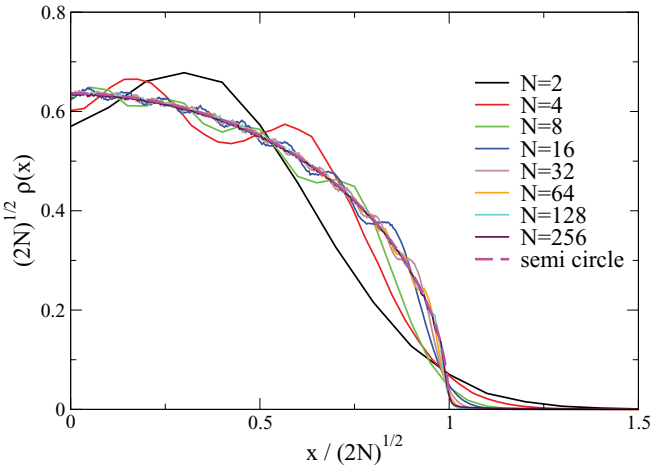

FIG. 2. (Color online) Scaling plot of one-particle density and comparison with its asymptotic form for large N, the Wigner semicircle law [thick dashed (magenta) line]. Only the positive half of the function, which is symmetric around $x = 0$, is shown.

Let us begin by discussing the one-particle density, $\rho(x) = \rho_1(x)/N$ [see Eq. (7)], which we choose to normalize so that it is the probability to find a particle at position x. This quantity is shown for several choices of particle number N in Fig. 1. The oscillations one can observe (most clearly for smaller particle number) are a clear sign of the correlation between the particles which would not be captured in a mean-field approach [23]. They are produced by the sum over Legendre functions in Eq. (7). With increasing N the distribution broadens and its height at $x = 0$ diminishes. Plotting this distributions in a double logarithmic fashion reveals that the final decay at large x is very steep (not shown). Asymptotically, for large N this distribution is known to approach the Wigner semicircle law [16,17] as can be deduced from the relation of the N-boson wave function to the N-fermion wave function. This relation predicts a scaling behavior of the one-particle density when plotting $\sqrt{2N}\rho(x)$ versus $x/\sqrt{2N}$ as is done in Fig. 2. For small N we see strong oscillations at small $x/\sqrt{2N}$ and the support of the density extends significantly beyond $x/\sqrt{2N} = 1$. With increasing number of bosons in the trap, the oscillations diminish and the support for the density reduces to $|x/\sqrt{2N}| \leqslant 1$. Taking into account the normalization we have chosen [i.e., $\int_{-\infty}^{\infty} \rho(x)dx = 1$], the prediction from the Wigner semicircle law reads for our case

$$\rho(x) = \frac{1}{\sqrt{2N}}\sqrt{\frac{2}{\pi}}\sqrt{1 - \frac{x^2}{2N}}, \tag{17}$$

which yields the dashed magenta line shown in Fig. 2.

So far, we have shown that simulating the trajectories generated by Eq. (16) and evaluating single-particle real-space properties reproduces the exactly known results for small N and the known asymptotic behavior for large N, and at a reasonable computational expense, as discussed in the appendix. Let us now turn to observables even more susceptible to the correlations within this bosonic system, which at the same time are also much harder to obtain by standard numerical approaches [15,17,30].

In Nelson's stochastic mechanics version of nonrelativistic quantum mechanics, particle positions are random variables with statistical properties fixed through Eq. (16). We have shown above that analyzing these properties is easily done for large particle numbers and that the results agree with what is known either analytically or by earlier numerically exact evaluations of the defining integrals over the ground-state wave function, which were, however, limited to significantly smaller particle numbers. From Eq. (16) we can also see that the osmotic velocities of the particles are random variables through their functional dependence on the position processes. In the original derivation of Eq. (16) [18] it was already shown that the first two moments of the osmotic momentum (in absence of a classical drift velocity field v) agree with the first two moments of the momentum operator in the standard mathematical representation of quantum mechanics. But what about the complete momentum distribution?

For the systems of linearly confined hard bosons this distribution has found much attention for the following reason: The reduced single-particle density matrix defined in Eq. (8) defines the natural orbitals $\Phi_j(x)$ (i.e., the effective single-particle states) through the following eigenvalue equation:

$$\int \rho_1(x,y)\,\Phi_j(y)\,dy = \lambda_j \Phi_j(x), \quad j = 0,1,2,\ldots. \tag{18}$$

The eigenvalues λ_j can be interpreted as the occupation numbers of the natural orbitals. When the occupation number λ_0 of the ground-state orbital scales linearly in the number of bosons, the system exhibits the coherence of a Bose-Einstein condensate (BEC). For the Tonks-Girardeau gas discussed here, it is known that λ_0 increases sublinearly in N [6]. Early on, bosons confined on a circle have been studied in detail [12–14]. This system is translationally invariant [i.e., we have $\rho_1(x,y) = \rho_1(x-y)$]. Fourier transforming Eq. (18) and using the definition of the momentum distribution in Eq. (9) then shows that the momentum distribution is identical to the distribution over the eigenvalues λ_j. In particular, the scaling behavior of the momentum distribution at $k = 0$ as

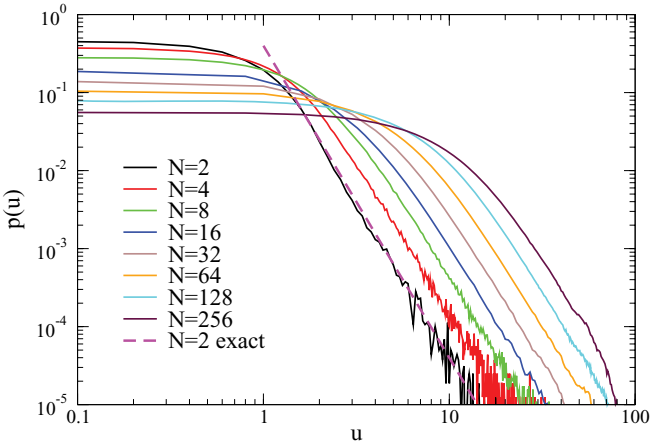

FIG. 3. (Color online) Momentum distribution for different numbers N of bosons (increasing from left to right) in a double-logarithmic presentation. The thick dashed (magenta) line is the exactly known asymptotic behavior for $N = 2$.

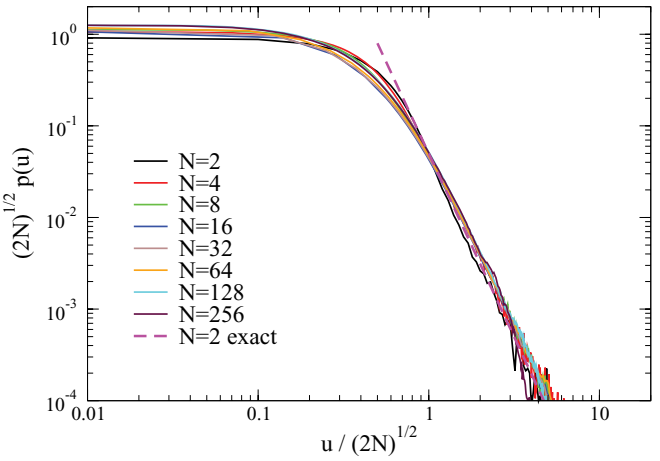

FIG. 4. (Color online) Scaled momentum distribution for different numbers N of bosons in a double-logarithmic presentation. The thick dashed (magenta) line is the exactly known asymptotic behavior for $N = 2$.

a function of N allows one to decide on the existence of a BEC. For the bosons in a harmonic trap we consider here, there is no translation invariance, so this relation does not hold. Consequently, the momentum distribution [15,30] and reduced density matrix [17] have been studied separately. We will focus in the following first on the behavior of the momentum distribution and then show that it still can be used to decide on the presence of a BEC.

In Fig. 3 we first display the probability distribution for the osmotic velocity u (only the part for $u > 0$ is shown, but the distribution is symmetric). In scaled variables for u this should coincide with the momentum distribution $n(k)$ from Eq. (9). As was calculated for $N = 2$ in Ref. [29] and predicted to hold for all N in Ref. [28] the distribution $p(u)$ asymptotically decays as u^{-4}. We resolve this behavior with the invested numerical effort here down to $p(u) \simeq 10^{-5}$. As is discussed in the appendix, the simulation effort at fixed number of integration steps increases as N^2, but at the same time, our statistics for $p(u)$ increases linearly in N. This is the reason for the smoother curves for larger N in Fig. 3. For $N = 256$, deviations from the u^{-4} behavior at large u are indicative of numerical subtleties in the integration of Eq. (16) which are also discussed in the appendix. Also included is the exact result for $N = 2$ shown by the thick dashed magenta line. For the normalization chosen here this reads

$$p(u) = \frac{1}{2}\sqrt{\frac{2}{\pi}}u^{-4}. \tag{19}$$

Clearly, the simulation results excellently reproduce this behavior. The virial theorem for the harmonic oscillator—classically as well as quantum mechanically—tells us that average kinetic energy equals average potential energy, $\langle p^2\rangle = \langle x^2\rangle$ in scaled coordinates. The inherent scale of $\sqrt{2N}$ we found for the extend of the real space density therefore should also govern the momentum space density. And consequently we should also have $p(u) \simeq (2N)^{-1/2}$ like for the real space density (see Fig. 2).

In Fig. 4 we plot the scaled probability $(2N)^{1/2}p(u)$ against the scaled momentum $u/(2N)^{1/2}$ and we clearly observe excellent scaling behavior in the asymptotic regime. The magenta line again shows the exact result for $N = 2$. For small momenta, the deviations from scaling, which is expected to hold only asymptotically, can be resolved, with the curves for small N deviating slightly from the large-N behavior. In Ref. [31] it was argued that this regime can be fit by Lévy-type distributions but due to the smallness of the fit range we did not try to perform this analysis here.

However, the perfect scaling observed in the asymptotic regime allows us to identify the prefactor for the asymptotic u^{-4} behavior for all N and not only for $N = 2$ as was done before. The observed scaling behavior implies

$$p(u) = \frac{1}{4}\sqrt{\frac{2}{\pi}}N^{3/2}u^{-4} \;\forall\; N, \tag{20}$$

generalizing the result known from the literature [29] for $N = 2$.

We already discussed that, for our nontranslationally invariant case, knowledge of the momentum distribution is not enough to determine the properties of the one-particle reduced matrix. The reason is that for $\rho_1(x,y) \neq \rho_1(x-y)$, the distribution $n(k)$ from Eq. (9) cannot be Fourier inverted to obtain $\rho_1(x,y)$. Let us define the true Fourier transform of the single-particle density matrix

$$n_1(k_1,k_2) = \frac{1}{2\pi}\int dx \int dy \rho_1(x,y)e^{-i(k_1x+k_2y)}. \tag{21}$$

This function can be inverted as

$$\rho_1(x,y) = \frac{1}{2\pi}\int dk_1 \int dk_2 n_1(k_1,k_2)e^{i(k_1x+k_2y)}. \tag{22}$$

From $n_1(k_1,k_2)$ we can obtain the momentum distribution as $n_1(k,-k) = n(k)$. Inserting the Fourier representation for the reduced density matrix into the eigenvalue equation (18) we obtain

$$\frac{1}{\sqrt{2\pi}}\int dk_1 \int dk_2 n_1(k_1,k_2)e^{ik_1x}\tilde{\Phi}_j(-k_2) = \lambda_j\Phi_j(x), \tag{23}$$

where $\tilde{\Phi}_j$ is the Fourier transform of Φ_j. Renaming $k_2 \to -k_2$ and performing a Fourier transform with respect to x we obtain

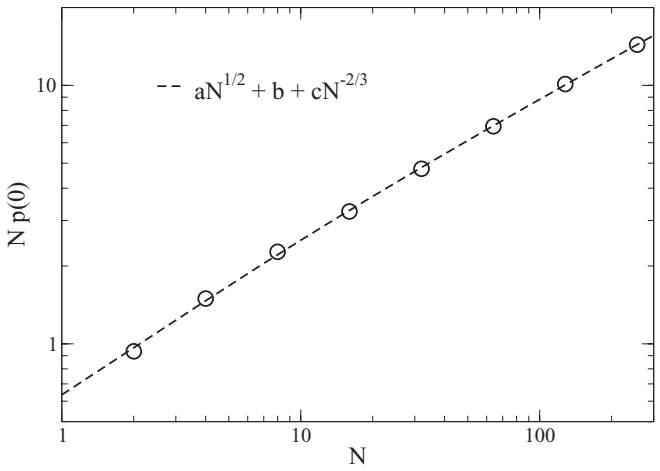

FIG. 5. Amplitude $p(0)$ of the momentum distribution at velocity $u = 0$ times particle number N as a function of N. The fit function is taken from Ref. [17]. The fit parameters are $a = 0.93$, $b = -0.45$, and $c = 0.156$.

using the completeness of the plain wave functions

$$\int dk_2 n_1(k, -k_2)\tilde{\Phi}_j(k_2) = \lambda_j \tilde{\Phi}_j(k). \tag{24}$$

The $\tilde{\Phi}_j$ are are effective single-particle states normalized in the L^2 norm. Therefore, the N-scaling of all λ_j is given by the N-scaling of the function $n_1(k, -k_2)$ and the same scaling relation must hold for all values of k we may choose in above equation, especially for $k = k_2$. This means that the scaling of all eigenvalues λ_j is determined by the scaling of the momentum distribution function $n(k)$, or $p(u)$ in our analysis. We already observed in Fig. 4 that this function obeys the same scaling behavior as the real-space density, meaning that its amplitude (when multiplied by N) asymptotically increases as $\sqrt{N}$, indicating the absence of BEC behavior in this system. For the occupation numbers of the natural orbitals the same scaling behavior was proven in Ref. [17] by a different argument. From the scaling plot in Fig. 4 it is also clear that we can in principle choose any value of k to study this scaling behavior. To follow the analysis performed for bosons on a ring, we plot in Fig. 5 the value $Np(0)$ as a function of N. The scaling behavior of the eigenvalues λ_0 and λ_1 was carefully studied in the analysis performed by Forrester *et al.* [17]. They were able to study particle numbers up to $N = 30$ and found that the following fit function described the approach to the asymptotic $\sqrt{N}$ behavior very well:

$$\lambda_j(N) = a\sqrt{N} + b + cN^{-z}, \tag{25}$$

where they found a best fit exponent $z = 2/3$ for $j = 0$ and $z = 4/3$ for $j = 1$. Our discussion above would indicate that the functional form of the approach to the asymptotic limit should be the same for all j. In Fig. 5 we include a fit in the form used for $j = 0$ by Forrester *et al.* [17], which describes our data perfectly well. A fit using $z = 4/3$ however, performs almost as well (it shows slightly larger deviations at small N) and leads to almost the same fit parameters ($a = 0.92$, $b = -0.41$, and $c = 0.152$). We therefore do not assign any significance to the value of z and argue that our analysis is, on the one hand, in perfect agreement with the one of Forrester *et al.* [17] and, on the other hand, strong evidence for our argument that also for the bosons trapped in a harmonic potential the scaling behavior of the momentum distribution can be used to determine the system-size scaling of the occupation numbers of the natural orbitals.

IV. CONCLUSION AND OUTLOOK

We have shown in this manuscript that the change of perspective offered by Nelson's stochastic mechanics approach to nonrelativistic quantum mechanics can be fruitfully applied to analyze the properties of a system of N hard-core bosons trapped in a harmonic potential. In the stochastic-mechanics approach, quantum mechanical observables are stochastic variables with distributions determined by a stochastic process for all position variables. These variables obey stochastic differential equations fixed by the wave function of the state one wants to analyze. We performed this analysis for the ground state of the bosonic system. It is noteworthy to recognize that once the wave function is known, a simulation of such a system proceeds in the same way as for a classical N-particle system. All observables are then just time averages along the system trajectory one generates from the equation of motion.

We have shown that in this approach we could reproduce known results for the one-particle density and its scaling behavior with respect to N. We were, however, able to extend the analysis to larger particle numbers than possible before. For the momentum distribution we revealed a scaling behavior and showed that the N dependence of the momentum distribution can be used to determine the N dependence of the occupation numbers of the natural orbitals, even for this system in a harmonic trap, where the reduced single-particle density is not translation invariant.

This method thus offers many opportunities for the detailed analysis of the physics of quantum systems for which either the exact or a good approximate wave function is known. It so far offers no way for the *ab initio* determination of the wave function of a quantum system and it remains a challenge to develop such a method.

ACKNOWLEDGMENT

The author is grateful to F. Rampf for many interesting discussions.

APPENDIX

In Sec. II we derived the following coupled stochastic differential equations (SDEs) for the system of hard core bosons:

$$dx_i(t) = \left[-x_i + \sum_{j=1, j\neq i}^{N} \frac{\mathrm{sgn}(x_j - x_i)}{|x_j - x_i|} \right] dt + dW_i(t). \tag{A1}$$

We will integrate this set of coupled equations employing a second-order Runge-Kutta scheme with a time-step $\Delta t = 0.0001$. The discrete Wiener increments $\Delta W_i(t)$ have to fulfill

$$\langle \Delta W_i(t) \rangle = 0 \text{ and } \langle \Delta W_i(t) \Delta W_i(t') \rangle = \delta(t - t')\Delta t. \tag{A2}$$

TABLE I. Run times of runs of 10^8 integration steps for Eq. (16).

N	2	4	8	16	32	64	128	256
t_{run} (min)	0.3	0.5	1.9	7.1	33.5	109	431	1720

To realize a second-order integrator for above set of SDEs, the increments $\Delta W_i(t)$ need not be Gaussian distributed with these first two moments, it suffices to employ uniform distributed random increments which have the same first four moments as this distribution [32]. This can be most efficiently done by generating uniformly distributed random numbers r_i in $[0,1]$ and setting

$$\Delta W_i(t) = \begin{cases} -\sqrt{3\Delta t}, & r_i < 1/6 \\ 0, & 1/6 < r_i < 5/6 \\ \sqrt{3\Delta t}, & r_i > 5/6. \end{cases} \tag{A3}$$

We have simulated systems of N hard bosons in a harmonic trap in this way, choosing $N = 2,4,8,16,32,64,128$, and 256. For $2 \leqslant N \leqslant 64$ we performed a number of runs of 10^9 integration steps, for $N = 128$ and $N = 256$ the run length was 10^8 integration steps. The simulation times for runs of 10^8 integration steps are given in Table I. The run times grow quadratically as a function of N, as expected from the sum over all pairs occurring in Eq. (16).

The integration step chosen above is rather small for the integration of a stochastic differential equation using a second-order algorithm. The reason for this choice becomes clear by looking at Fig. 6 which displays the momentum distributions for $N = 32$ and $N = 128$ obtained using $\Delta t = 10^{-3}$ and $\Delta t = 10^{-4}$.

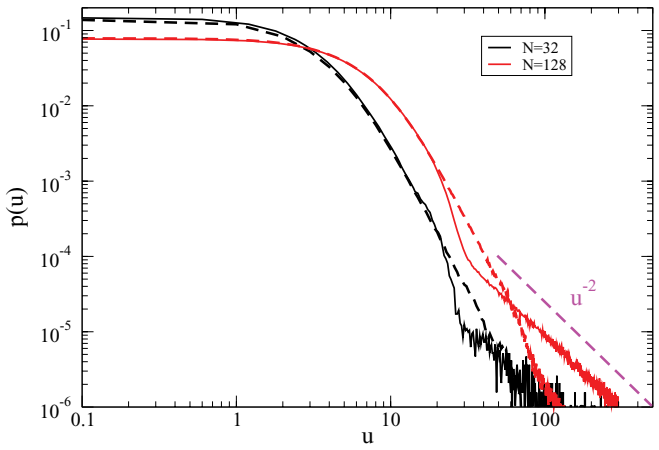

FIG. 6. (Color online) Momentum distribution for $N = 32$ (black curves) and $N = 128$ [red (light gray) curves] using $\Delta t = 10^{-3}$ (full curves) and $\Delta t = 10^{-4}$ (dashed curves), respectively. The thick dashed line indicates a u^{-2} law.

For the larger integration time step we observe a crossover to a u^{-2} behavior at large u or small $p(u)$, respectively. This is an artefact of the discretization which vanishes choosing a smaller time step. To be more precise, the crossover is shifted to ever smaller values of $p(u)$. At the same time, this artefact also introduces a crossover to a x^{-2} behavior in the density distribution (not shown) with $\rho(x) = p(u)$ (in scaled dimensionless variables) for large x (u). This artefact can be traced to the behavior of the bosons at the surface of the system. Clearly, these are (instantaneously) not equivalent to the particles in the center of the system, although the wave function is, of course, symmetrized with respect to the particle indices. Following the trajectory of every particle, however, makes these surface effects visible. The physical interpretation of these effects awaits further study.

[1] I. Bloch, J. Dalibard, and W. Zwerger, Rev. Mod. Phys. **80**, 885 (2008).
[2] M. H. Anderson, J. R. Ensher, M. R. Mathews, C. E. Wieman, and E. A. Cornell, Science **269**, 198 (1995).
[3] C. C. Bradley, C. A. Sackett, J. J. Tollett, and R. G. Hulet, Phys. Rev. Lett. **75**, 1687 (1995).
[4] K. B. Davis, M.-O. Mewes, M. R. Andrews, N. J. van Druten, D. S. Durfee, D. M. Kurn, and W. Ketterle, Phys. Rev. Lett. **75**, 3969 (1995).
[5] L. Pitaevskii and S. Stringari, *Bose-Einstein Condensation* (Oxford University Press, Oxford, 2003).
[6] D. S. Petrov, G. V. Shlyapnikov, and J. T. M. Walraven, Phys. Rev. Lett. **85**, 3745 (2000).
[7] T. Kinoshita, T. Wenger, and D. S. Weiss, Science **305**, 1125 (2004).
[8] B. Paredes, A. Widera, V. Murg, O. Mandel, S. Fölling, J. I. Cirac, G. V. Shlyapnikov, T. W. Hänsch, and I. Bloch, Nature (London) **429**, 277 (2004).
[9] E. P. Gross, Nuovo Cimento, Suppl. **20**, 454 (1961); L. P. Pitaevskii, Sov. Phys. JETP **13**, 451 (1961).
[10] M. A. Cazalilla, R. Citro, T. Giamarchi, E. Orignac, and M. Rigol, Rev. Mod. Phys. **83**, 1405 (2011).
[11] M. Girardeau, J. Math. Phys. **1**, 516 (1960).
[12] A. Lenard, J. Math. Phys. **5**, 930 (1964); **7**, 1268 (1966).
[13] B. Sutherland, Phys. Rev. A **4**, 2019 (1971); J. Math. Phys. **12**, 246 (1971); Phys. Rev. A **5**, 1372 (1972).
[14] H. G. Vaidya and C. A. Tracy, Phys. Rev. Lett. **42**, 3 (1979); **43**, 1540 (1979); J. Math. Phys. **20**, 11 (1979).
[15] T. Papenbrock, Phys. Rev. A **67**, 041601(R) (2003).
[16] T. H. Baker and P. J. Forrester, Commun. Math. Phys. **188**, 175 (1997).
[17] P. J. Forrester, N. E. Frankel, T. M. Garoni, and N. S. Witte, Phys. Rev. A **67**, 043607 (2003).
[18] E. Nelson, Phys. Rev. **150**, 1079 (1976).
[19] E. Nelson, *Quantum Fluctuations* (Princeton University Press, Princeton, 1985).
[20] M. McClendon and H. Rabitz, Phys. Rev. A **37**, 3479 (1988); H. Nitta and T. Kudo, *ibid.* **77**, 014102 (2008).
[21] M.-Q. Chen and M. S. Wang, Phys. Lett. A **149**, 441 (1990); K. Imafuku, I. Ohba, and Y. Yamanaka, *ibid.* **204**, 329 (1995).

[22] M. D. Girardeau, E. M. Wright, and J. M. Triscari, Phys. Rev. A **63**, 033601 (2001).
[23] E. B. Kolomeisky, T. J. Newman, J. P. Straley, and X. Qi, Phys. Rev. Lett. **85**, 1146 (2000).
[24] P. Vignolo, A. Minguzzi, and M. P. Tosi, Phys. Rev. Lett. **85**, 2850 (2000).
[25] M. Brack and M. V. N. Murthy, J. Phys. A **36**, 1111 (2003).
[26] J. Roccia, M. Brack, and A. Koch, Phys. Rev. E **81**, 011118 (2010).
[27] M. Olshanii and V. Dunjko, Phys. Rev. Lett. **91**, 090401 (2003).
[28] G. Moreno, Phys. Lett. A **373**, 3897 (2009).
[29] A. Minguzzi, P. Vignolo, and M. P. Tosi, Phys. Lett. A **294**, 222 (2002).
[30] G. J. Lapeyre Jr., M. D. Girardeau, and E. M. Wright, Phys. Rev. A **66**, 023606 (2002).
[31] A. V. Ponomarev, S. Denisov, and P. Hänggi, Phys. Rev. A **81**, 043615 (2010).
[32] B. Dünweg and W. Paul, Int. J. Modern Phys. C **2**, 817 (1991).